Chemical models of genetic toggle switches

Patrick B. Warren[1,2] and Pieter Rein ten Wolde[2,3]

[1] *Unilever R&D Port Sunlight, Bebington, Wirral, CH63 3JW, United Kingdom*
[2] *FOM Institute for Atomic and Molecular Physics, Kruislaan 407, 1098 SJ Amsterdam, The Netherlands.*
[3] *Division of Physics and Astronomy, Vrije Universiteit, De Boelelaan 1081, 1081 HV Amsterdam, The Netherlands*

(Dated: September 30, 2004)

We study by mean-field analysis and stochastic simulations chemical models for genetic toggle switches formed from pairs of genes that mutually repress each other. In order to determine the stability of the genetic switches, we make a connection with reactive flux theory and transition state theory. The switch stability is characterised by a well defined lifetime τ. We find that τ grows exponentially with the mean number $\overline{N}$ of transcription factor molecules involved in the switching. In the regime accessible to direct numerical simulations, the growth law is well characterised by $\tau \sim \overline{N}^{\alpha}\exp(b\overline{N})$, where α and b are parameters. The switch stability is decreased by phenomena that increase the noise in gene expression, such as the production of multiple copies of a protein from a single mRNA transcript (shot noise), and fluctuations in the number of proteins produced per transcript. However, robustness against biochemical noise can be drastically enhanced by arranging the transcription factor binding domains on the DNA such that competing transcription factors mutually exclude each other on the DNA. We also elucidate the origin of the enhanced stability of the exclusive switch with respect to that of the general switch: while the kinetic prefactor is roughly the same for both switches, the 'barrier' for flipping the switch is significantly higher for the exclusive switch than for the general switch.

PACS numbers: 05.40.-a; 87.16.Yc

I. INTRODUCTION

In an organism, genes can be turned on or off by the binding of proteins to regulatory sites on the DNA in the vicinity of the starting point for transcription [1]. The proteins are known as transcription factors and the DNA binding sites are known as operators. The process is an example of gene regulation. Transcription factors can turn genes off by stereochemical blockage of the binding of RNA polymerase (RNAp), or they can turn genes on by co-operative binding (recruitment) of RNAp [1].

Since transcription factors are proteins, they are coded for elsewhere on the genome. This means that transcription factors can regulate the production of other transcription factors, or indeed can regulate their own production. A highly complex network of biochemical reactions can be built up, capable, in principle, of solving arbitrarily complex computational problems [2, 3]. The network is interfaced to the outside world by, e.g., signalling cascades from receptor proteins or by specific interactions between transcription factors and small molecules such as metabolites. In this way, even relatively simple organisms such as *E. coli* can perform fairly complex computations such as integrating different environmental signals. In higher organisms, gene regulation networks lie at the heart of cell differentiation and developmental pathways.

Genetic toggle switches are an informative paradigm in this context [4, 5]. They are regulatory constructs which select between two possible stable states, representing for example differentiation between two developmental pathways. Perhaps the simplest kind of switch is one that is constructed from a pair of genes that mutually repress each other, as indicated in Fig. 1. The switch of λ-phage in *E. coli* is a naturally occuring example, which has been studied in much detail [4, 6, 7, 8]. Another well-known example is that of the human herpesvirus 3 (chickenpox or varicella-zoster virus), which has a pathogenesis that is remarkably similar to λ-phage; the virus lies dormant after the initial infection, but can be triggered to re-emerge much later as shingles (herpes zoster). Synthetic toggle switches have also been constructed *in vivo* [9].

Genetic switches are usually flipped by external signals. In the λ-phage , for example, the switch is initially in the dormant (lysogenic) state but can be flipped into the active (lytic) state by the presence of the bacterial protein RecA. Such an induction event occurs when the cell starts to produce RecA to repair DNA damage as a result of, e.g., a burst of UV light.

Importantly, genetic switches are often so stable that they remain in one state until the external trigger flips the switch. In wild-type λ-phage spontaneous flips are extremely rare, occurring at a rate of perhaps as low as one spontaneous flip in 10^{12} s [8]. An important question, therefore, is: what are the design principles that allow the switch to attain such extreme stability in the presence of fluctuations and biochemical noise? This question is particularly relevant, because detailed modelling has suggested that the stability of λ-phage cannot be explained on the basis of our current understanding [8].

We have recently shown that mutual exclusion of competing transcription factors can drastically enhance the stability of genetic switches [10]. Transcription factors

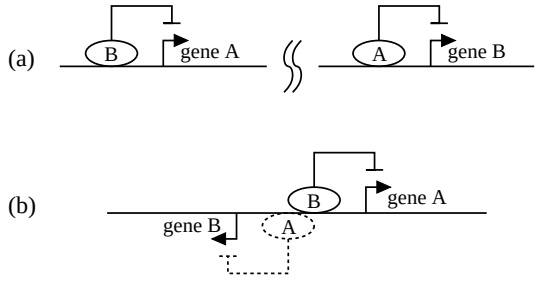

FIG. 1: (a) A genetic toggle switch can be formed from a pair of genes that mutually repress each other's expression. (b) If the genes are transcribed on opposite strands of the DNA, the upstream regulatory domains can overlap and interfere with one another. As a result, competing regulatory molecules mutually exclude each other.

can mutually exclude each other, if their operator sites (partially) overlap (see Fig. 1b). It appears that nature has exploited the functional benefit of this spatial arrangement of operators, since a recent statistical analysis has revealed that this network motif of 'overlapping operons' is over-represented in the bacterium *E. coli* [11].

In this paper, we extend the analysis of Ref. 10 in several ways [12]. In the next section, we first describe the set of chemical reactions by which we model the genetic toggle switches (see Fig. 1). We then turn to a mean-field (chemical rate equation) analysis of the appearance of switching behaviour. This mean-field analysis shows that the region of bistability is significantly larger for the exclusive switch than for the general switch. In order to determine the life times of the stable steady states of the switches, we have performed direct stochastic simulations; these are described in section IV. We then consider a number of refinements of the basic switch model. In particular, we explicitly take into account transcription and translation. We show that both 'shot noise' and fluctuations in the number of proteins produced per mRNA transcript markedly decrease the switch stability. However, we again find that the exclusive switch is still orders of magnitude more stable than the general switch. In this paper, we also elucidate the origin of the enhanced stability of the exclusive switch with respect to that of the general switch: while the kinetic prefactor is roughly the same for both switches, the 'free-energy' barrier for flipping is significantly higher for the exclusive switch than for the general switch [10]. This underscores our earlier observation that mutual exclusion can drastically enhance the robustness of genetic switches to biochemical noise [10]. It also strongly supports the conjecture that regulatory control is one of the main evolutionary driving forces that shape the organisation of genes and operons on the genome [11].

II. MODEL SPECIFICATION

Our starting point is a set of chemical reactions which model the processes involved in the toggle switches shown in Fig. 1. As chemical species, we introduce a pair of transcription factors (TFs) which can exist as monomers, A and B, or multimers, A_n and B_m. The multimers are responsible for regulating gene expression and are allowed to bind to the genome at an operator site. Multimers are introduced in order to get sufficient co-operativity in the binding isotherms to make a genetic switch [13], as described in more detail below. The state of the operator is represented by O, OA_n, *etc*, depending on the state of binding of the multimers. The chemical reactions are

$$n\mathrm{A} \rightleftharpoons \mathrm{A}_n, \quad m\mathrm{B} \rightleftharpoons \mathrm{B}_m, \qquad (k_\mathrm{f}, k_\mathrm{b}) \qquad (1a)$$

$$\mathrm{O} + \mathrm{A}_n \rightleftharpoons \mathrm{OA}_n, \quad \mathrm{O} + \mathrm{B}_m \rightleftharpoons \mathrm{OB}_m, \qquad (k_\mathrm{on}, k_\mathrm{off}) \qquad (1b)$$

$$\mathrm{OA}_n + \mathrm{B}_m \mid \mathrm{OB}_m + \mathrm{A}_n \rightleftharpoons \mathrm{OA}_n\mathrm{B}_m, \qquad (k_\mathrm{on}, k_\mathrm{off}) \qquad (1c)$$

$$\mathrm{O} \mid \mathrm{OA}_n \hookrightarrow \mathrm{A}, \quad \mathrm{O} \mid \mathrm{OB}_m \hookrightarrow \mathrm{B}, \qquad (k_\mathrm{A}), (k_\mathrm{B}) \qquad (1d)$$

$$\mathrm{A} \mid \mathrm{B} \rightarrow \emptyset, \qquad (\mu_\mathrm{A}), (\mu_\mathrm{B}) \qquad (1e)$$

Here we have adopted a condensed notation in which '|' indicates alternative sets of reactants and '$\hookrightarrow$' indicates that the reactants are not destroyed by the reaction. For example the first of Eqs. (1d), $\mathrm{O} \mid \mathrm{OA}_n \hookrightarrow \mathrm{A}$, represents two reactions $\mathrm{O} \rightarrow \mathrm{O} + \mathrm{A}$ and $\mathrm{OA}_n \rightarrow \mathrm{OA}_n + \mathrm{A}$.

The reactions in Eqs. (1) account for, respectively, the formation of multimers, the binding of TF multimers to the operator (Eqs. (1b) and (1c)), the expression of TF monomers, and the degradation of TF monomers. Repression of gene expression is implicit in Eqs. (1d), thus A is expressed if and only if B_m is not bound, *etc*. Reaction rates are as indicated, and we define equilibrium constants for multimerisation, $K_\mathrm{d} = k_\mathrm{f}/k_\mathrm{b}$, and operator binding, $K_\mathrm{b} = k_\mathrm{on}/k_\mathrm{off}$.

Whilst detailed and biologically faithful models can be constructed as has been done for the λ-phage switch [6, 8], the above model is intentionally as simple as possible. We believe that such an approach is as important as detailed biological modelling in elucidating the basic physical principles behind switches. Thus, for example, we have condensed the details of transcription and translation into a single reaction step in Eqs. (1d), governed by rate coefficients k_A and k_B. In a later section we explore the possibility of refining the model at this point.

It should be noted, however, that the design of the network has to obey certain constraints. In particular, the TFs must bind co-operatively to the DNA in order to make a working switch [13]. In the present model, co-operativity is introduced through the binding of TF multimers rather than monomers.

In our model the operator is in one of four states $\{\mathrm{O}, \mathrm{OA}_n, \mathrm{OB}_m, \mathrm{OA}_n\mathrm{B}_m\}$. We now include the effect of interference between the upstream regulatory domains by disallowing some of these states. This is in the spirit of simplicity, strictly speaking the effect is to modify the probabilities of the states. Since the empty operator state

TABLE I: Distinct possibilities for the subsets of operator states for our switch model: '0' indicates the state is disallowed, '1' indicates it is allowed.

operator states	O	OA_n	OB_m	OA_nB_m
case		α	β	γ
general	1	1	1	1
exclusive	1	1	1	0
partially co-operative	1	1	0	1
totally co-operative	1	0	0	1

is always a possibility and both A_n and B_m should be allowed to bind otherwise they would not be TFs, it turns out that there are only five possibilities, two of which are related by symmetry. The four distinct cases are shown in Table I, and are implemented by excluding some of the reactions in Eqs. (1b) and (1c). For example, the exclusive switch is obtained by discarding the reactions in Eqs. (1c) thereby removing the state OA_nB_m.

III. MEAN-FIELD ANALYSIS

We first analyse the behaviour of Eqs. (1) using chemical rate equations. This plays the role of a mean field theory for this problem since chemical rate equations describe the temporal evolution of the mean concentrations of molecules. Switching behaviour corresponds to the appearance of two distinct stable fixed points (attractors) in the space of concentration variables. For the general switch, the problem has been analysed in detail by Cherry and Adler [13]. For the exclusive switch, a specific example has been studied by Kepler and Elston [14]. Our approach is a generalisation of the analysis of Cherry and Adler.

Let us consider what happens for A. Write n_A for the number of A monomers in the cell *etc*, and let the cell volume be V_c. In a steady state, the multimerisation reaction $nA \rightleftharpoons A_n$ is in equilibrium and

$$\left(\frac{n_{A_n}}{V_c}\right) = K_d \left(\frac{n_A}{V_c}\right)^n. \tag{2}$$

Similarly the binding reaction $O + A_n \rightleftharpoons OA_n$ (if it is allowed) is in equilibrium and

$$\left(\frac{n_{OA_n}}{V_c}\right) = K_b \left(\frac{n_O}{V_c}\right)\left(\frac{n_{A_n}}{V_c}\right). \tag{3}$$

Now, n_O is the probability that the operator is in state O times the number of copies of the genome in the cell (usually assumed to be one), *etc*. Therefore

$$\frac{\text{Prob}(OA_n)}{\text{Prob}(O)} = \frac{K_b K_d}{V_c^n}\,[n_A]^n \equiv x^n \tag{4}$$

where we have introduced x as a reduced concentration variable, equal to $(1/V_c)(K_bK_d)^{1/n}$ times the number of monomers of A in the cell. Similarly we introduce a reduced concentration variable y for the number of monomers of B.

¿From the totality of binding equilibria, we surmise that the probabilities of the operator states $\{O, OA_n, OB_m, OA_nB_m\}$ are in the ratio $1 : \alpha x^n : \beta y^m : \gamma x^n y^m$ where we have covered off all the switch construction possibilities by introducing a set of coefficients (α, β, γ) which take the values zero or one according to Table I. The probability of the operator being in a state where A is expressed is therefore

$$f(x,y) = \frac{1+\alpha x^n}{1+\alpha x^n + \beta y^m + \gamma x^n y^m}, \tag{5}$$

and of being in a state where B is expressed is

$$g(x,y) = \frac{1+\beta y^n}{1+\alpha x^n + \beta y^m + \gamma x^n y^m}. \tag{6}$$

For A, expression occurs at a rate k_A and degradation at a rate $\mu_A \times n_A$. It is convenient to define a reduced degradation rate

$$\tilde{\mu}_A = \frac{V_c}{(K_bK_d)^{1/n}}\,\frac{\mu_A}{k_A}. \tag{7}$$

If there is more than one copy of the genome in the cell, we should additionally divide by the number of copies of the genome. A similar reduced degradation rate $\tilde{\mu}_B$ is defined for B.

At a fixed point (a steady state), the rate of expression is equal to the rate of degradation (for example $k_A f = \mu_A n_A$), for both TFs. Using the reduced concentrations and degradation rates defined above, the steady states are defined by

$$f(x,y) = \tilde{\mu}_A x, \quad g(x,y) = \tilde{\mu}_B y. \tag{8}$$

We see that the steady states only depend on $\tilde{\mu}_A$ and $\tilde{\mu}_B$.

The simplest way to proceed now is to consider the fixed points for the dynamical system

$$\dot{x} = f(x,y) - \tilde{\mu}_A x, \quad \dot{y} = g(x,y) - \tilde{\mu}_B y. \tag{9}$$

This is only an approximation to the full dynamics, since it assumes that TF binding is always in equilibrium. However, Cherry and Adler demonstrate under a mild restriction that the fixed points for Eqs. (9) correspond to the possible fixed points of the full system. The mild restriction is that, under the full dynamics, if the concentration of one of the TFs is held fixed, the concentration of the other TF should settle on a unique value. This holds for our switch problem.

Switching behaviour corresponds to the existence of two stable fixed points for Eqs. (9), separated by a third fixed point which is unstable in one direction, like a transition state. Thus a test for switching behaviour is whether the dynamical system in Eqs. (9) admits an unstable fixed point which is unstable in one direction.

From dynamical systems theory, this can be determined by considering the determinant of the stability matrix

$$\mathbf{M} = \begin{pmatrix} f_x - \tilde{\mu}_\mathrm{A} & f_y \\ g_x & g_y - \tilde{\mu}_\mathrm{B} \end{pmatrix} \tag{10}$$

where $f_x = \partial f/\partial x$, *etc.* The required test is that $\det \mathbf{M} < 0$ at the fixed point in question. At a fixed point, one can eliminate $\tilde{\mu}_\mathrm{A}$ and $\tilde{\mu}_\mathrm{B}$ between Eqs. (8) and (10). We find that $\det \mathbf{M} = (1/xy) \times D$ where we have introduced the discriminant function

$$D(x,y) = (f - xf_x)(g - yg_y) - (xg_x)(yg_y). \tag{11}$$

The sign of D mirrors the sign of $\det \mathbf{M}$ so that if $D < 0$ at a fixed point, that fixed point is unstable in one direction. Moreover, for any point in the (x, y) plane, D has a definite value independent of the values of $\tilde{\mu}_\mathrm{A}$ and $\tilde{\mu}_\mathrm{B}$. Thus in the plane of reduced concentration variables, the nature of a fixed point is determined solely by its position. In particular, the region $D < 0$ contains all the unstable fixed points of the kind desired, and only those kind of fixed points. This region is bounded by the line $D = 0$.

Normally one regards the parameters k_A, *etc*, as given, and one has to solve Eqs. (8) for the position of any fixed points. However, if one knows a fixed point (x, y) in the plane of reduced concentration variables, the corresponding reduced parameters are given by $\tilde{\mu}_\mathrm{A} = f/x$ and $\tilde{\mu}_\mathrm{B} = g/y$, from Eqs. (8). The region $D < 0$ in the (x, y) plane is therefore mapped to a region (a wedge) in the $(\tilde{\mu}_\mathrm{A}, \tilde{\mu}_\mathrm{B})$ plane. Fig. 2 shows two examples. Note that the mapping from (x, y) to $(\tilde{\mu}_\mathrm{A}, \tilde{\mu}_\mathrm{B})$ is triple-valued within the wedge, since for parameters where switching behaviour occurs there are two stable fixed points in addition to the unstable fixed point.

An interesting analogy with a fluid-fluid demixing transition in a binary liquid mixture can be made at this point since both are examples of a cusp catastrophe [15]. In this analogy, $\tilde{\mu}_\mathrm{A}^{-1}$ and $\tilde{\mu}_\mathrm{B}^{-1}$ correspond to the chemical potentials of the two components and the wedge $D < 0$ to the region of spinodal instability. The cusp of the wedge in Fig. 2(b) would correspond to the critical point.

We now apply the above analysis to the switch models of the preceding section. Firstly, for $n = m = 1$, one can prove that $D > 0$ for all four kinds of switch in Table I. This confirms the result of Cherry and Adler, namely that some form of co-operativity is required to make a working switch.

Secondly, the discriminant for the totally co-operative case turns out to simplify to $D = (1 + z)[1 + (m + n)z]$ where $z = x^n y^m$. This is positive for all values of n and m. Thus switching behaviour cannot occur for the totally co-operative switch.

For the remaining cases, we have analysed in detail the situation for *dimerising* switches, with $n = m = 2$. The details of this analysis are given in Appendix A. Fig. 2 shows the regions in the both the (x, y) and $(\tilde{\mu}_\mathrm{A}, \tilde{\mu}_\mathrm{B})$ planes where switching behaviour occurs, for the general and exclusive switches. Clearly there is a more extensive region of switching behaviour in the $(\tilde{\mu}_\mathrm{A}, \tilde{\mu}_\mathrm{B})$ plane for the exclusive case compared to the general case. Switching behaviour is strongly suppressed for the partially co-operative cases; for example if OB_2 is disallowed, switching occurs only if $\tilde{\mu}_\mathrm{A} \lesssim 0.1$ and $\tilde{\mu}_\mathrm{B} \lesssim 0.01$ (lines not shown in Fig. 2). Thus we conclude that, at least in mean field theory, restricting the set of operator states can have a marked effect on the possibility to form a genetic switch.

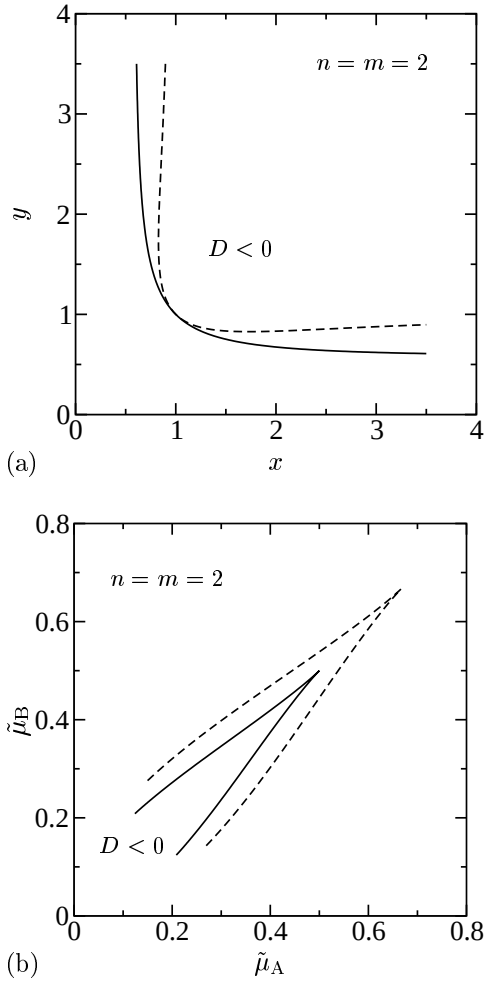

FIG. 2: In mean field theory, switching behaviour is confined to a region in the (x, y) plane in (a), or equivalently to a wedge in the $(\tilde{\mu}_\mathrm{A}, \tilde{\mu}_\mathrm{B})$ plane in (b). Results are shown for dimerising general (solid line) and exclusive (dashed line) switches. Note that the bistable region is larger for the exclusive switch than for the general switch.

IV. STOCHASTIC SIMULATIONS

Whilst mean field theory indicates the regions in parameter space where switching might occur, it has nothing to say about the switch stability and the effects of

TABLE II: Rate coefficients and equilibrium constants for a representative set of the reactions which define the baseline model. Here V_c is the cell volume and k is used as a unit of (inverse) time.

reaction	baseline		
$O \to O + A$	k		
$A \to \emptyset$	μ	$(0.2\text{–}0.8)\,k$	
$2A \to A_2$	k_f	$5kV_c$	
$A_2 \to 2A$	k_b	$5k$	$K_d = k_f/k_b = V_c$
$O + A_2 \to OA_2$	k_{on}	$5kV_c$	
$OA_2 \to O + A_2$	k_{off}	k	$K_b = k_{on}/k_{off} = 5V_c$

number fluctuations in systems with a finite size. To address these problems, we therefore turn to a stochastic simulation of the chemical reactions in Eqs. (1). This is done via the 'Gillespie' algorithm [16], which is a kinetic Monte Carlo scheme [17] to generate trajectories in the space of concentration variables appropriate to the chemical master equation.

Since these simulations are quite intensive, we focus again on the dimerising general and exclusive switches, and on the symmetry line $\mu_A = \mu_B = \mu$ and $k_A = k_B = k$. We additionally have to supply values for all the rate coefficients in Eqs. (1). To do this, we regard $k \approx 0.1$–$1\,s^{-1}$ (the expression rate) as a unit of (inverse) time, and μ (the degradation rate) as the main control variable. As is the case with biological systems, real rate coefficients vary over quite a range of values. The baseline parameter set is biologically motivated, with expression being a slow step and binding equilibrium biased in favour of bound states. Rate coefficients for our baseline model for a representative set of reactions are given in Table II. For comparison, literature values for λ-phage can be found in Arkin *et al* [6], in Aurell *et al* [7, 8], and in Bundschuh *et al* [18]. The rate coefficients for bimolecular reactions, such as the forward dimerisation and forward binding reactions, have units of volume divided by time. Since our concentrations are expressed as the number of molecules in the cell volume, the natural units for these rate coefficients are kV_c where $V_c \approx 2\,\mu m^3$ ($1/V_c \approx 1\,nM$) is the cell volume. For the baseline parameters, the mean-field theory predicts bistability for $\mu/k < \sqrt{5}/2 = 1.12$ for the general switch and $\mu/k < 2\sqrt{5}/3 = 1.49$ for the exclusive switch. The implementation of the Gillespie algorithm with concentrations expressed as the number of molecules in the cell is straightforward.

In the next section, we will first focus on the steady-state properties of both switches. In the subsequent section, we will address the dynamics of switching.

A. 'Free-energy' landscapes

We monitor the total number of molecules of A and B in the cell, N_A and N_B. These include the monomers, the free dimers, and the bound dimers (see for example Eq. (A15)). This is motivated primarily by the observation by Bialek that the switch lifetime is likely to be an exponential function of the number of molecules involved in the switching process [19]. Moreover, N_A and N_B are the relevant slow variables in the sense of Bundschuh *et al* [18].

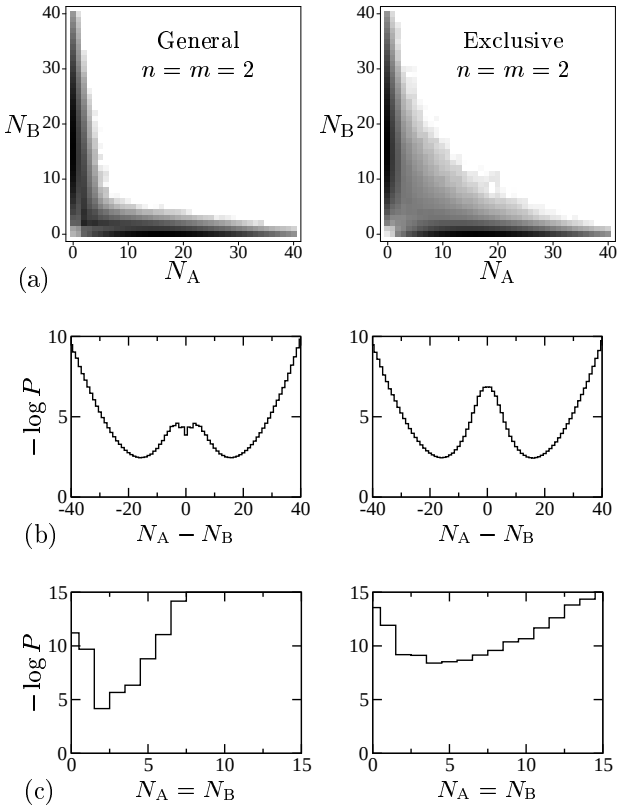

FIG. 3: (a) Probabilities in (N_A, N_B) plane constructed from trajectories of total duration $kt \approx 8 \times 10^6$, for general and exclusive switches, at $\mu = 0.4\,k$. Greyscale is logarithmic from $P \leq 10^{-7}$ (white) to $P \geq 0.04$ (black). (b) Probabilities collapsed onto the $N_A - N_B$ line, plotted as a dimensionless 'free energy' $-\log P$; the maximum at $N_A = N_B$ corresponds to the mean-field transition state. (c) Probabilities along the diagonal line $N_A = N_B$; the minimum in this section now corresponds to the mean-field transition state. It is seen that the saddle-point of the exclusive switch is higher than that of the general switch. See also Table III for locations of the features in $P(N_A, N_B)$ and the barrier heights.

To demonstrate the appearance of switching, we can construct the probability distribution $P(N_A, N_B)$ for states in the (N_A, N_B) plane. This is done by generating a sufficiently long Gillespie trajectory to obtain good coverage of all the interesting features of the probability distribution [12]. Fig. 3 shows the main features for $\mu = 0.4\,k$, for both the dimerising general and exclusive switches with this direct method.

We see that switching appears as a double maximum in the probability distribution, and there is a

TABLE III: Locations of maxima and transition states for $P(N_\mathrm{A}, N_\mathrm{B})$ for dimerising general (DGS) and exclusive (DES) switches at $\mu = 0.4\,k$ (Fig. 3), compared to fixed points from mean field theory (MFT, section III and appendix A).

		Maximum		Transition state
		N_A	N_B	$N_\mathrm{A} = N_\mathrm{B}$
DGS	Gillespie	15.0 ± 0.5	0	2 ± 1
($\gamma = 1$)	MFT	16.91	0.09	5.74
DES	Gillespie	15.0 ± 0.5	0	4 ± 1
($\gamma = 0$)	MFT	16.04	0.16	3.15

transition state at a low number of molecules for both TFs; we *assume* here that the transition state corresponds to the saddle point in the 'free-energy landscape' $-\log[P(N_A, N_B)]$. Table III contains the locations of the probability maxima and the transition state, comparing the Gillespie results with the mean-field theory fixed point solutions of the preceeding section. The maxima are in quite good agreement with the mean-field fixed points, although there is some difference in the location of the saddle-point. The first column in Table IV shows the probability of reaching states with $N_\mathrm{A} = N_\mathrm{B}$ determined from Fig 3. This probability is an order of magnitude lower for the exclusive switch than for the general switch, which indicates that the exclusive switch is more stable than the general switch.

Fig. 4 shows the mean number of molecules of the most-expressed transcription factor as a function of μ/k in the switching regime, for the two kinds of switch. We define this *via* the time average

$$\overline{N} = \overline{\max(N_\mathrm{A}, N_\mathrm{B})}. \tag{12}$$

Since the system spends most of the time near a stable state, this average is dominated by the number of molecules in the stable states. As such, the time average can be compared to the mean field stable fixed point. Further, in the stable steady states both switches should behave very similarly (see Eq. 1). Fig. 4 shows that while the average number of molecules $\overline{N}$ is indeed nearly the same for the two switches, it also lies systematically a little above the mean field theory prediction.

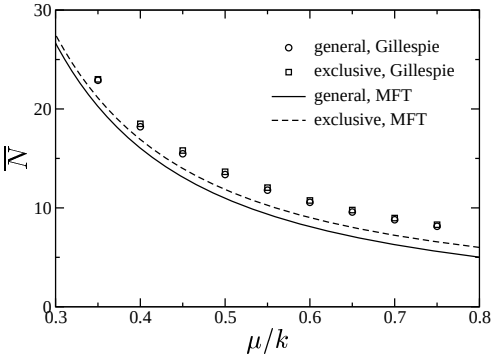

FIG. 4: Mean copy number of most-expressed TF, as a function of the degradation rate, for both kinds of switch and baseline parameters. 'Gillespie' refers to the results of the stochastic simulations and 'MFT' refers to those of the mean-field analysis described in section III.

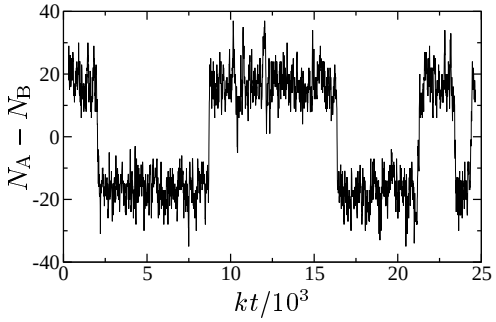

FIG. 5: Typical time series for $N_\mathrm{A} - N_\mathrm{B}$. Data is for the dimerising exclusive switch at $\mu = 0.4\,k$.

B. Rate constants

We now turn to the switch *dynamics*. Fig. 5 shows typical time series for $N_\mathrm{A} - N_\mathrm{B}$ for the dimerising exclusive switch at $\mu = 0.4\,k$. The appearance of the two switch states where one of the TFs is strongly repressed compared to the other one is clearly seen. These correspond to the probability maxima of Fig. 3(a). A switching event occurs when the roles of the two TFs flip spontaneously.

In order to elucidate the stability of the switches, we make a connection with the reactive flux method that has been pioneered by Bennett [20] and Chandler [21] and that is now widely used in the field of soft-condensed matter physics [22]. We first define an order parameter, q, that serves as our reaction coordinate and measures the progress of flipping the switch from one state to the other. In what follows, we will take $q = N_A - N_B$. Furthermore, we define two characteristic functions that indicate in which state the system is in:

$$\begin{aligned} h_A(q) &= 1,\ q < q^* && (13)\\ &= 0,\ q \geq q^* && (14)\\ h_B(q) &= 0,\ q < q^* && (15)\\ &= 1,\ q \geq q^*. && (16) \end{aligned}$$

It is natural to take for q^* the value that corresponds to the top of the 'barrier' that separates the two stable steady sates. We have thus chosen $q^* = 0$ for both switches (see Fig. 3).

We now assume that we can make a separation of time scales [22]. In particular, we assume that there exists a time t that is longer than the time t_trans it takes for transient behavior to relax, but shorter than the characteristic time t_rxn for making a transition from one state

of the switch to the other. If this assumption holds, then we can coarse-grain the switch as a two-state system. If the flipping on the time scale $t_{\rm rxn}$ is a Poisson process, then the relaxation of the switch is given by the following expression

$$\frac{\overline{h_A(0)h_B(t)}}{\overline{h_A}} = \overline{h_B}\left(1-\exp[-(k_{AB}+k_{BA})t]\right). \quad (17)$$

Here, the overbar denotes a time average; contributions to the average are weighted according to the stationary distribution of states. The expression on the left-hand side yields the probability that the switch is in state B at time t, given that initially it was in state A. If this time t is longer than $t_{\rm trans}$ and if there are no correlations between successive switching events on this time scale, then this correlation function should be given by the macroscopic expression on the right-hand side of the above equation, where k_{AB} and k_{BA} are the rate constants for flipping the switch in the forward and backward directions, respectively. The above relation thus only holds for $t > t_{\rm trans}$.

It is instructive to take the time derivative in Eq. 17. This yields

$$\frac{\overline{h_A(0)\dot{h}_B(t)}}{\overline{h_A}} = \overline{h_B}(k_{AB}+k_{BA})\exp[-(k_{AB}+k_{BA})t]. \quad (18)$$

If we now consider times t smaller than $t_{\rm rxn} = 1/(k_{AB}+k_{BA})$, but larger than $t_{\rm trans}$, and exploit the detailed balance condition $\overline{h_B}/\overline{h_A} = k_{AB}/k_{BA}$, then we find

$$\frac{\overline{h_A(0)\dot{h}_B(t)}}{\overline{h_A}} = k_{AB}. \quad (19)$$

This shows that the flux of trajectories from A to B should exhibit a plateau for times $t_{\rm trans} < t < 1/(k_{AB}+k_{BA})$. Indeed, the macroscopic switching rate is precisely given by the constant flux of trajectories in this regime.

In general, however, it is useful to define a time dependent rate constant:

$$\begin{aligned} k_{AB}(t) &= \frac{\overline{h_A(0)\dot{h}_B(t)}}{\overline{h_A}} && (20)\\ &= \frac{\overline{\dot{q}(0)\delta(q(0)-q^*)\theta(q(t)-q^*)}}{\overline{\theta(q^*-q(t))}} && (21)\\ &= \frac{\overline{\delta(q-q^*)}}{\overline{\theta(q^*-q(t))}}\,\frac{\overline{\dot{q}(0)\delta(q(0)-q^*)\theta(q(t)-q^*)}}{\overline{\delta(q-q^*)}} && (22)\\ &= P_0(q^*)\,\overline{\dot{q}(0)\theta(q(t)-q^*)}^* && (23)\\ &= P_0(q^*)\,R(t). && (24)\end{aligned}$$

Here, θ is the Heaviside function. The overline with the asterix * denotes an average over states at the top of the barrier.

It is seen that $k(t) = k_{AB}(t)$ is the product of two contributions. The first is $P_{\rm o}(q^*)$, which is given by,

$$P_0(q^*) = \frac{P(q^*)}{\sum_{-\infty}^{q^*} P(q)}. \quad (25)$$

Here $P(q)$ is the steady-state probability of finding the system with a reaction coordinate of size q. Noting that if $q < q^*$ the system is in the initial state, it is clear that $P_{\rm o}(q^*)$ is the probability of finding the system at the top of the barrier divided by the probability of finding it in the initial state. This quantity can be directly obtained from Fig. 3, and is shown in Table IV.

The second contribution to $k(t)$ is $R(t)$, which gives the average flux of trajectories at the top of the barrier. As explained in [21], the *initial* rate $k(t \to 0^+)$ corresponds to the approximation for the rate constant in the transition state theory of chemical reactions:

$$k_{\rm TST} = k(t\to 0^+) = P_0(q^*)\,\overline{\dot{q}(0)\theta(\dot{q})}^*. \quad (26)$$

Transition-state theory assumes that all trajectories initially heading from the top of the barrier towards the final state will indeed end up in the final state and all trajectories initially heading towards the initial state will end up in the initial state. This assumption is only correct if no trajectories recross the barrier. In the present case, recrossing turns out to be quite significant and, as a result, $k(t)$ will be significantly lower than $k_{\rm TST}$. It is conventional to express the reduction of $k(t)$ due to recrossings in terms of the transmission coefficient $\kappa(t)$, defined as

$$\kappa(t) \equiv \frac{k(t)}{k_{\rm TST}} = \frac{R(t)}{R(0^+)} \quad (27)$$

where $R(0^+) = \overline{\dot{q}(0)\theta(\dot{q})}^*$. We note that, just as $k_{AB}(t)$ exhibits a plateau value for $t_{\rm trans} < t < t_{\rm rxn} = 1/(k_{AB}+k_{BA})$, $\kappa(t)$ and $R(t)$ also reach a constant value on this time scale. We will simply refer to them as the transmission coefficient κ and kinetic prefactor R, respectively.

For many rare event problems in soft-condensed matter, it is not feasible to obtain the rate constant by calculating the correlation function $\langle h_A(0)h_B(t)\rangle$ in a long, brute-force simulation. In order to alleviate the rare event problem, a widely used approach is to first calculate the free-energy barrier $P_o(q^*)$ using umbrella sampling [23] and then compute the kinetic prefactor $R(t)$ by shooting-off (molecular dynamics) trajectories from the top of the barrier [20, 21]. However, the umbrella sampling technique in its conventional form relies on an energy-functional and is therefore only applicable to systems that obey detailed balance. Biochemical networks are usually out of equilibrium and consequently lack detailed balance. In Appendix B, we show that the genetic toggle switches considered here also do not obey detailed balance. We can therefore not use the Bennett-Chandler approach [20, 21]. Indeed, we have resorted to long, brute-force simulations in order to calculate the flipping rates for the toggle switches. To be more precise [12], we have obtained the rate constant by fitting the correlation function $\overline{h_A(0)h_B(t)}/\overline{h_A}$ to its macroscopic expression as given by Eq.17; for the symmetric switches considered here, $k_{AB} = k_{BA} = 1/\tau$, where τ is the life time of the stable steady state. In practice, to reduce noise in the correlation function, we excise a window of states around

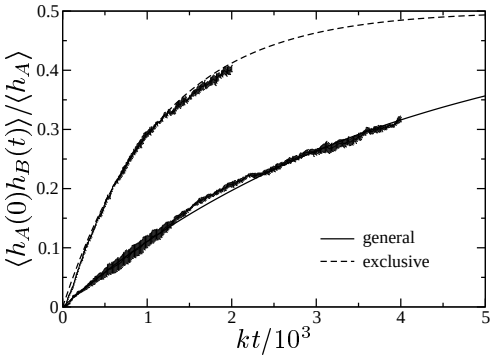

FIG. 6: The cross correlation between the indicator functions $h_A = \theta(q_A - q(t))$ and $h_B = \theta(q(t) - q_B)$ allows an accurate determination of the switch lifetime. Results are shown for the general and exclusive switches at $\mu = 0.4\,k$, with $-q_A = q_B = 5$. The lines are fits to Eq. (17) in the form $\langle h_A(0)h_B(t)\rangle/\langle h_A\rangle = (1 - \exp[-2t/\tau])/2$. Table IV contains the corresponding values of τ.

q^* and define $h_A = \theta(q_A - q(t))$ and $h_B = \theta(q(t) - q_B)$ where $q_A < q^*$ and $q_B > q^*$. Most of our calculations have been performed for $-q_A = q_B = 5$, but we find that, as expected, our results are insensitive to the precise values chosen, provided that the system is well into the switching regime where there is a good separation of time scales. Fig. 6 shows typical correlation functions.

In Fig. 7 we show the switch lifetime $\tau = 1/k_{AB}$ ($= 1/k_{BA}$ for the symmetric switches) as a function of the mean value of the most-expressed TF for both kinds of switches, as μ varies. We see that τ grows extremely rapidly with $\overline{N}$, which is the basic reason why extremely stable switches can be built with only a few hundred expressed proteins. Our simulations cover $10 \lesssim \overline{N} \lesssim 30$, but if we extrapolate our results to $\overline{N} \approx 100$, then $k\tau \approx 10^7$ for the general switch but $k\tau \approx 10^{11}$ for the exclusive switch. In the latter case, this corresponds to lifetimes measured in tens of years. Such extremely long lifetimes have been reported for λ-phage [8]. Equally important, Fig. 7 is a dramatic confirmation that the switch construction has a marked influence on stability. The exclusive switch lifetime grows much more rapidly with the mean copy number than the general switch lifetime.

We find that τ grows sub-exponentially with $\overline{N}$ and can be fit to a functional form suggested by analysis of a related problem, namely that of switching between broken-symmetry phases in a driven diffusive model [24, 25]. The fit is to $\tau = A\overline{N}^{\alpha}\exp(b\overline{N})$, where $A = 50.4$, $\alpha = 0.72$, $b = 0.097$ for the general switch, and $A = 7.32$, $\alpha = 1.16$, $b = 0.19$ for the exclusive switch. This fit gives quantitative support to Bialek's conjecture that the switch lifetime grows exponentially with the number of molecules involved in the switching process [19], but additionally indicates that there is a logarithmic correction in $\overline{N}$.

Table IV shows the barrier heights $P_o(q^*)$ computed from the direct numerical simulations of $P(N_{\rm A}, N_{\rm B})$. We

TABLE IV: Switching kinetics. The first column is the probability of reaching the top of the barrier from Fig. 3, the second column is the lifetime from Fig. 6, and the third column is kinetic prefactor defined to be $R = 1/(P_0(q^*)\tau)$. The fourth column is the mean escape rate $R(0^+)$ to $N_{\rm A} > N_{\rm B}$ from $N_{\rm A} = N_{\rm B}$ as determined from additional analysis of the simulations, and the final column is the transmission coefficient $\kappa = R/R(0^+)$. A figure in brackets after a result is an estimate of the error in the final digit of that result.

	$P_0(q^*)/10^{-3}$	$k\tau/10^3$	R/k	$R(0^+)/k$	κ
DGS	9(1)	2.3(2)	0.048(7)	0.24(1)	0.20(3)
DES	0.92(1)	8.0(5)	0.14(1)	0.98(4)	0.14(1)

can now obtain the kinetic prefactor R by dividing the rate constant $k_{AB} = 1/\tau$ by $P_o(q^*)$: $R = k_{AB}/P_o(q^*)$ (see also Eq. 24). We find that the underlying barrier-crossing rate $R \approx 0.05 - 0.15k$ is a (small) fraction of k, which corresponds to the time scale for gene expression (see Table II). In fact, for the general switch, the kinetic prefactor R is significantly lower than the slowest reaction in the system, which is the degradation reaction with $\mu = 0.2 - 0.8k$ (see also Table II). Since R can be interpreted as the rate at which the barrier is crossed (i.e., the flux of trajectories at the top of the barrier), it is clear that crossing the barrier typically involves a large number of protein synthesis and degradation steps.

We have also directly computed from the Gillespie trajectories the distribution of escape times from the dividing surface $N_{\rm A} = N_{\rm B}$ to states with $N_{\rm A} \neq N_{\rm B}$. We find that for both kinds of switches, the escape time distribution is quite well approximated by a Poisson distribution with a characteristic lifetime $\tau_{\leftrightarrow}$. Since the switches are symmetric, this means we can define the escape rate to one side (for example to $N_{\rm A} > N_{\rm B}$) to be $R(0^+) = 1/2\tau_{\leftrightarrow}$. Estimates for $R(0^+)$ from the Poisson-distribution fit are shown in the fourth column

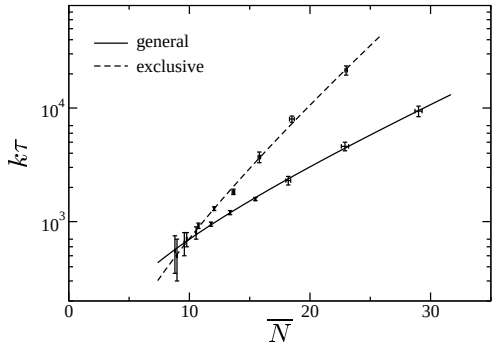

FIG. 7: Switch lifetime as a function of the mean number of the most-expressed TF. The exclusive switch becomes orders of magnitude more stable than the general switch at high numbers of the expressed TF. The lines are fits to $\tau \sim \overline{N}^{\alpha}\exp(b\overline{N})$ as discussed in the text.

in Table IV. The ratio of the barrier crossing rate to the one-sided escape rate is the transmission coefficient, $\kappa = R/R(0^+)$ [22]. As Table IV shows, the transmission coefficient for both kinds of switch is 10–20%. This shows that the barrier crossing is quite diffusive. In other words, a typical transition path between the two stable regions crosses and re-crosses the top of the barrier $N_{\rm A} = N_{\rm B}$ several times before committing to one of the stable basins. This is in accord with our findings on the statistics of $q = 0$ crossing times reported previously [10]. It is also consistent with the observation that a typical transition path involves many protein synthesis and degradation reactions.

V. BEYOND THE BASELINE MODEL

We now consider the effects of varying parameters away from the baseline set, and changing some other aspects such as introducing a more detailed representation of transcription and translation. Switch stability is generally unaffected by variation of the kinetic rates that do not alter the mean copy number of the TFs. What does have an effect, as we shall see, are phenomena which increase the 'shot noise' in expression. These include the generation of multiple copies of the TF from each mRNA transcript and stochastic fluctuations in the number of copies of the TF generated per mRNA transcript.

In this section we give results for the dimerising exclusive switch. We have repeated all the simulations for the dimerising general switch and we find that the same trends are recovered. We also find that the exclusive switch is *always* markedly more stable than the corresponding general switch, in a manner represented by Fig. 7.

A. Varying parameters away from baseline

Fig. 8 shows that the switch lifetime is very insensitive to variations away from the baseline kinetic parameters that do not affect the mean field steady states. If, however, we vary the kinetic parameters such that the mean field steady states are changed, then we do see a systematic change in the switch stability. For instance, the switch stability is enhanced if the binding equilibrium is moved in favour of bound TF by increasing $k_{\rm on}$ (the rate of binding to DNA). This is because the number of molecules of each TF at the point where switching just starts decreases as $K_{\rm b} = k_{\rm on}/k_{\rm off}$ increases (see Eq. (A16)), and thus at fixed $\overline{N}$ we are effectively moving deeper into the bistable region. This leads to a more stable switch.

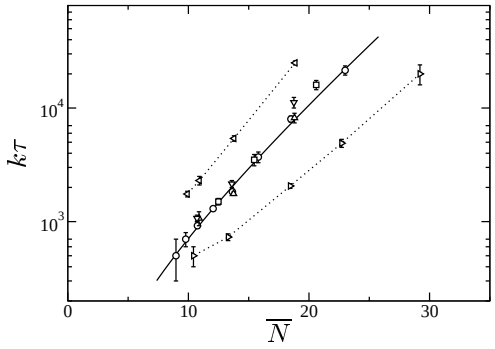

FIG. 8: Switch lifetime for the dimerising exclusive switch as some of the baseline kinetic parameters are varied. Data is shown for baseline model (circles; see Table II), with the number of copies of the genome doubled and expression rate halved (squares), with $k_{\rm f}$ and $k_{\rm b}$ doubled (up triangles), with $k_{\rm on}$ and $k_{\rm off}$ doubled (down triangles), with $k_{\rm on} = 10kV_{\rm c}$ and, as before, $k_{\rm off} = k$ (left triangles), and with $k_{\rm on} = 2kV_{\rm c}$ and, as before, $k_{\rm off} = k$ (right triangles); see Table II for the meaning of the rate constants. The solid line is the fit to the baseline data from Fig. 7.

B. Effect of messenger RNA

We have condensed the various steps in gene expression into a single 'expression reaction' in Eqs. (1d). In reality, however, many steps are involved. We now analyse these steps in more detail. Recall that the genetic information is first *transcribed* into messenger RNA (mRNA), then *translated* into proteins by ribosomes. It is often the case that several copies of the protein can be generated from one mRNA transcript. In the simplest way, we can capture this by replacing Eqs. (1d) by a version in which r copies of each transcription factor are generated from each mRNA transcript, thus

$$\mathrm{O} \mid \mathrm{OA}_n \hookrightarrow r_{\rm A} \times \mathrm{A}, \quad \mathrm{O} \mid \mathrm{OB}_m \hookrightarrow r_{\rm B} \times \mathrm{B}. \tag{28}$$

It is easy to see that nothing changes in mean field theory provided that $r_{\rm A}k_{\rm A}$ and $r_{\rm B}k_{\rm B}$ are used in place of $k_{\rm A}$ and $k_{\rm B}$. We have undertaken simulations for the case $r_{\rm A} = r_{\rm B} = 2$ and $k_{\rm A} = k_{\rm B} = k/2$, which in mean field theory is identical to our baseline. However, as Fig. 9 shows, the switch lifetime is decreased as a result of having TFs generated two at a time. The basic reason is that the 'shot noise' in the expression reactions has increased.

Even if on average one TF is produced from each mRNA transcript, noise can arise from the fluctuations about this mean, as we now discuss. To capture this, we explicitly include the generation and degradation of mRNA for the two TFs in the list of chemical reactions. The expression reactions in Eq. (1d) are replaced by the following reactions:

$$\mathrm{O} \mid \mathrm{OA}_n \hookrightarrow \mathrm{M_A} \to \emptyset, \qquad (k'_{\rm A}), (\mu'_{\rm A}) \tag{29a}$$
$$\mathrm{O} \mid \mathrm{OB}_m \hookrightarrow \mathrm{M_B} \to \emptyset, \qquad (k'_{\rm B}), (\mu'_{\rm B}) \tag{29b}$$
$$\mathrm{M_A} \hookrightarrow \mathrm{A}, \quad \mathrm{M_B} \hookrightarrow \mathrm{B}. \qquad (k''_{\rm A}), (k''_{\rm B}) \tag{29c}$$

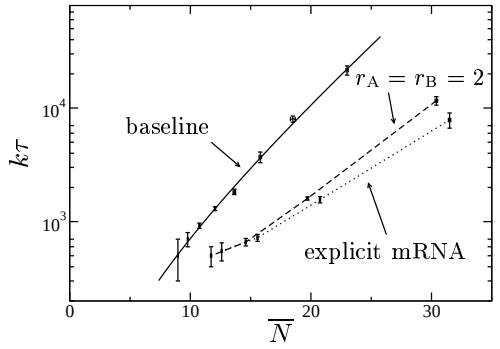

FIG. 9: Switch stability is degraded if multiple copies of the TF are produced in each expression reaction, in this case $r_A = r_B = 2$ in Eq. (28). In a model which includes explicit mRNA production (as described by Eqs. (29)), then even if on average only one TF is produced per transcript, the stability is similarly degraded by fluctuations about the mean. 'Baseline' refers to the baseline model, as described in Table II.

In these, M_A and M_B are the mRNA species, and the reactions represent the generation and degradation of mRNA, and the translation of mRNA into TFs. We have introduced new rate coefficients for the translation, transcription and mRNA degradation steps.

In a steady state in mean field theory, the rate of transcription balances the rate of mRNA degradation and the mean number of mRNA transcripts is k'/μ'. Each transcript produces TFs at a rate k'', hence the overall rate of production of TF is $(k'/\mu') \times k''$. We conclude that the equivalent expression rate is

$$k = \frac{k'k''}{\mu'}. \tag{30}$$

Going beyond mean field theory, the statistics of this basic model for mRNA translation can be solved exactly [26, 27]. Translation occurs at a rate k'' and degradation at a rate μ', hence the probability per unit time of either a translation or a degradation event taking place is $k'' + \mu'$. Given that an event has taken place, the probability that it was a translation event is $p = k''/(k'' + \mu')$ and the probability that it was a degradation event is $q = 1 - p = \mu'/(k'' + \mu')$. Therefore, the probability that r copies of the protein are generated before the mRNA transcript is degraded is $P_r = qp^r$. From this, all the statistics can be calculated. For instance, the mean number of TFs produced per transcript is $\langle r \rangle = \sum_{r=0}^{\infty} rP_r = p/q = k''/\mu'$, which agrees with the expectation from Eq. (30). Also $\langle r^2 \rangle = p/q^2$, so that the standard deviation divided by the mean is $\sqrt{q/p} = \langle r \rangle^{-1/2}$. Thus there is considerable noise due to fluctuations in the number of proteins generated per transcript, and this noise is largest when the mean number of TFs produced per transcript is small.

To see the effect of this noise we have implemented the additional reactions in Eqs. (29) in our reaction schemes and again determined the switch lifetimes by direct simulation. Fig. 9 shows the results for $k''_A = k''_B = 5k'_A = 5k'_B = \mu'_A = \mu'_B = 5k$. For these parameter values $k''_A k'_A/\mu'_B = k''_B k'_B/\mu'_B = 1$ and, according to Eq. (30), such a system should be identical to our baseline. Moreover since $k''_A/\mu'_A = k''_B/\mu'_B = 1$, there is on average one TF produced per mRNA transcript, so the 'shot noise' associated with the mean number of TFs produced per transcript is the same as in the baseline model. However, the simulations clearly demonstrate that the additional noise due to fluctuations about this mean reduces the switch lifetime considerably.

C. Expression as a multistep process

As a second refinement to the model for gene transcription and translation, we now consider gene expression as a multistep process. We thus replace the single reaction $O \to O + A$ by a sequence of reaction steps

$$O \to O_1 \to O_2 \to O_3 \to \cdots \to O_n \to O + A. \tag{31}$$

If there is only one intermediate stage, O_1 say, this can be used to model the formation of an 'open complex' [28]. If there are multiple intermediate stages, this could represent the individual steps of the RNA polymerase that walks along the DNA, or those of the ribosomes that walk along the mRNA. In some of the more detailed models of gene expression, all these intermediate steps are captured in detail [6].

We can make a connection with the baseline model by computing the waiting time for the lumped reaction $O \to O + A$. Since the waiting times for the individual steps in Eq. (31) are independent statistical quantities, the waiting time for the whole sequence is the sum of the waiting times for the individual steps. In terms of reaction rates, $1/k = \sum 1/k_i$, where k is the rate of the lumped reaction, and the k_i are the rates of the intermediate steps.

It follows that the waiting time distribution for the lumped reaction is not a Poisson distribution. Indeed the central limit theorem indicates that the lumped reaction will tend to have a Gaussian distribution of waiting times, effectively converging on a δ-function for a very large number of steps. Thus the approximation which replaces Eq. (31) by $O \to O + A$ amounts to replacing the true non-Poisson distribution of waiting times by a Poisson distribution with the same mean.

We have tested the consequences of this assumption for two cases. In the first test, we have inserted a single intermediate stage in Eq. (31) to represent the formation of the open complex. The rates of the two steps were chosen to be $(5/4)k$ and $5k$, so that formation of the open complex is the slow step. With this choice, the rate for the lumped reaction is the same as the baseline model. In the second test, we have inserted four intermediate stages in the reaction scheme, so that there are five intermediate reaction steps between O and O+A, to model for example

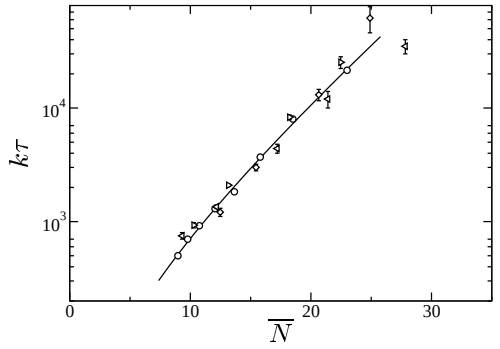

FIG. 10: Compared to the baseline model (circles; see Table II), there is practically no effect on switch stability when one activation step is included (right triangles) or several are included (left triangles) as in Eq. (31) (see main text for details). There is also little change if the operator is 'split' as in Fig. 11 and Eqs. (32) (diamonds). The line is the fit to the baseline data from Fig. 7.

the progressive stages of transcription. We have chosen the rates of these intermediate steps all equal to $5k$ so again the effective rate for the lumped reaction is the same as the baseline model. However, the sum of the variances for the individual steps is now five times smaller than the variance in the waiting time for the lumped reaction.

Fig. 10 shows data for the dimerising exclusive switch with these modifications. It shows that the switch stability is practically unaffected by the inclusion of the additional reaction steps. These results suggest that the precise waiting time statistics for these multistep reactions are less important for the switch stability than the statistics of the number fluctuations (as studied in considerable detail in the preceeding section). This is perhaps not so surprising, since the activation process to flip the switch must proceed by multiple coincidences of the 'right' expression or degradation events (see also discussion on kinetic prefactor R in section IV B), and so the detailed waiting time statistics of the individual reaction steps are unimportant.

D. Can the operator be split?

The basic premise of the exclusive switch is that the binding of one TF excludes the binding of the other TF. Whilst it is natural to think of this in terms of a diverging pair of genes on opposite strands of the DNA as shown in Fig. 1(b), it is also possible to achieve the same effect by having each TF prevent the binding of the other TF at separated operators on the DNA. An exclusive switch with such a 'split' arrangement is shown in Fig. 11. This arrangement is interesting because for each gene, one TF regulates expression by acting as a repressor, but the other TF acts only indirectly by preventing binding of

FIG. 11: A 'split' exclusive switch can be built out of distinct operators provided each TF blocks the other TF from binding, at each operator site.

the repressor TF.

We can set up a system of chemical reactions to model the split operator case as follows. Suppose that $\mathrm{O_A}$ and $\mathrm{O_B}$ denote the operator sites for the genes which code for A and B, respectively. Then the set of reactions is

$$\mathrm{O_A} + \mathrm{A}_n \rightleftharpoons \mathrm{O_A A}_n, \quad \mathrm{O_A} + \mathrm{B}_m \rightleftharpoons \mathrm{O_A B}_m, \tag{32a}$$
$$\mathrm{O_B} + \mathrm{A}_n \rightleftharpoons \mathrm{O_B A}_n, \quad \mathrm{O_B} + \mathrm{B}_m \rightleftharpoons \mathrm{O_B B}_m, \tag{32b}$$
$$\mathrm{O_A} \mid \mathrm{O_A A}_n \hookrightarrow \mathrm{A}, \quad \mathrm{O_B} \mid \mathrm{O_B B}_m \hookrightarrow \mathrm{B}, \tag{32c}$$

plus the multimerisation and degradation reactions from Eqs. (1). We assume that the rates for all binding and unbinding reactions are k_{on} and k_{off}, and those for expression of A and B are k_{A}, and k_{B}, respectively. This set of reactions describes the split analogue of the exclusive switch. In mean field theory, this model is identical to the standard case. We have simulated this model and indeed find that there is little alteration to the switch stability, as shown in Fig. 10.

We conclude that it is the exclusive nature of the TF binding which makes the exclusive switch markedly more stable than the general case. This can be achieved by overlapping the operator sites of genes that are arranged in a divergent manner and (thus) on opposite strands of the DNA as in Fig. 1(b), or by the pure exclusive binding arrangements of Fig. 11. It appears, however, that nature has taken advantage of the elegance of the former scenario: in *E. coli* there are a significantly large number of diverging gene pairs with overlapping operator sites [11].

VI. DISCUSSION

A genetic switch is inherently stochastic, because of the molecular character of its components. Our simulations demonstrate that the stability of a genetic switch can be strongly influenced by its construction. If the competing transcription factors mutually exclude each other at the operator regions, then the switch stability is markedly enhanced. Mutual exclusion of competing regulatory molecules can be obtained by overlapping operons, a network motif that we have recently identified in a statistical analysis of the gene regulatory network of *E. coli* [11].

The basic conclusion that mutual exclusion of competing regulatory molecules can strongly enhance the stability of biochemical networks is robust. Nevertheless,

the switch stability is influenced by phenomena that increase the noise in gene expression. Such phenomena include the generation of multiple copies of a transcription factor from the same mRNA transcript, as well as intrinsic noise arising from the fluctuations in the numbers of proteins produced from a transcript.

When expressed as a function of the number of molecules involved in switching, the switch stability is characterised by a well defined lifetime τ which grows exponentially with the mean number, $\overline{N}$, of the transcription factors that are involved in the switching. In the regime accessible to direct numerical simulations, the growth law is well characterised by $\tau \sim \overline{N}^{\alpha}\exp(b\overline{N})$, where and α and b are parameters.

Whereas we have investigated a number of details that might affect switch stability, we have left out some considerations which might additionally be important. Foremost amongst these is the influence of cell division and the cell cycle. Other effects such as fluctuations in the availability of RNA polymerase and ribosomes might also have an influence on switch stability. Another aspect that should be investigated is the response of the switch to a perturbation, in other words how one might toggle a switch by introducing a pulse of some kind. We leave all these questions to future work.

The rapid increase of the switch stability with the number of expressed transcription factors presents a fundamental limitation to the use of direct simulation to compute the switch lifetime. This provokes the question: is there a smarter way to compute the switch stability for long-lived switches? Such simulation methods would generically be useful since the characterisation of rare events remains a key challenge in computational systems biology [29]. In the field of soft-condensed matter physics, numerical techniques, such as the reactive flux method [20, 21] and transition path sampling [30], have been developed that make it possible to simulate rare events such as crystal nucleation, protein folding and chemical reactions. Biochemical networks, however, differ fundamentally from these problems. In the former problems, the stationary distribution of states is usually known beforehand. Indeed, these systems typically obey detailed balance. In contrast, our genetic circuits, like most biochemical networks, do not satisfy detailed balance. This means that the stationary distribution of states is not known *a priori*. As a result, numerical techniques developed to tackle rare events in the field of soft-condensed matter physics, cannot straightforwardly be transposed to biochemical networks. Recently, we have developed a new numerical technique, called Forward Flux Sampling [31], that does not rely upon prior knowledge of the stationary distribution of states. The scheme is easily applicable to a wide variety of biochemical switches, such as that of bacteriophage lambda, and makes it possible to calculate rates of switching and to identify patwhays for switching. The technique should therefore lead to a better understanding of these rare, but important events in biology.

VII. ACKNOWLEDGEMENTS

We thank Rosalind Allen and Daan Frenkel for useful discussions and for a critical reading of the manuscript, and Martin Evans for drawing our attention to the work on driven diffusive systems. We thank Nick Buchler for drawing our attention to the 'split' operator arrangement shown in Fig. 11. We are also grateful to the hospitality of the Kavli Institute for Theoretical Physics in Santa Barbara, where part of the work was carried out. This research was supported in part by the National Science Foundation under Grant No. PHY99-07949. This work is supported by the Amsterdam Centre for Computational Science (ACCS). The work is part of the research program of the "Stichting voor Fundamenteel Onderzoek der Materie (FOM)", which is financially supported by the "Nederlandse organisatie voor Wetenschappelijk Onderzoek (NWO)".

APPENDIX A: MEAN FIELD THEORY FOR DIMERISING SWITCHES

Here are the explicit results of the mean field (chemical kinetics) analysis for the dimerising switches. Firstly consider the general switch. For this case, $\alpha = \beta = \gamma = 1$, and Eqs. (5) and (6) simplify to $f = 1/(1+y^2)$ and $g = 1/(1+x^2)$. The discriminant equation $D = 0$ solves to

$$y^2 = \frac{x^2+1}{3x^2-1}. \tag{A1}$$

and requires $x > 1/\sqrt{3} \approx 0.577$ for solutions. The cusp of the wedge in the $(\tilde{\mu}_{\rm A}, \tilde{\mu}_{\rm B})$ plane lies at the point $\tilde{\mu}_{\rm A} = \tilde{\mu}_{\rm B} = 1/2$ and corresponds to the point $x = y = 1$ on the line $D = 0$.

For the exclusive switch ($\alpha = \beta = 1$, $\gamma = 0$) Eqs. (5) and (6) give $f(x,y) = (1+x^2)/(1+x^2+y^2)$ and $g(x,y) = f(y,x)$. The discriminant equation $D = 0$ now solves to

$$y^2 = \frac{\pm\sqrt{x^8+14x^6+25x^4-24x^2} - x^4 - 5x^2 + 2}{2(x^2-1)} \tag{A2}$$

This requires $x > \sqrt{(3\sqrt{17}-11)/\sqrt{2}} \approx 0.827$ for solutions, at which point $y = \sqrt{3} \approx 1.73$. The curve for $x > 1$ corresponds to the positive sign; one can show that the curve for $x < 1$ can be generated by reflecting the curve for $x > 1$ through the line $x = y$ (the curve passes through $x = y = 1$). Also, $y \to 1$ as $x \to \infty$. The cusp of the wedge in the $(\tilde{\mu}_{\rm A}, \tilde{\mu}_{\rm B})$ plane lies at the point $\tilde{\mu}_{\rm A} = \tilde{\mu}_{\rm B} = 2/3$, again corresponding to the point $x = y = 1$ on the line $D = 0$.

Finally consider the partially co-operative switch. This has a much reduced range of switching behaviour and the corresponding lines have not been shown in Fig. 2. Consider the case where OB_2 is disallowed. In this case ($\alpha = \gamma = 1$, $\beta = 0$) Eqs. (5) and (6) give $f = (1+$

$x^2)/(1+x^2+x^2y^2)$ and $g = 1/(1+x^2+x^2y^2)$. The discriminant equation $D=0$ solves to

$$y^2 = \frac{(x^2+1)^2}{x^2(x^2-5)} \tag{A3}$$

and requires $x > \sqrt{5} \approx 2.24$ to have a solution. The cusp of the wedge in the $(\tilde{\mu}_\mathrm{A}, \tilde{\mu}_\mathrm{B})$ plane corresponds to the point $x = \sqrt{(13+\sqrt{129})/\sqrt{2}} \approx 3.49$ and $y = \sqrt{(51+13\sqrt{129})/10} \approx 1.41$, and lies at $\tilde{\mu}_\mathrm{A} = \sqrt{(491-43\sqrt{129})/16} \approx 0.101$ and $\tilde{\mu}_\mathrm{B} = \sqrt{(1591\sqrt{129}-18057)/192} \approx 0.0190$.

We now describe the mean field fixed points for dimerising exclusive and general switches along the symmetry line $\mu_\mathrm{A} = \mu_\mathrm{B} = \mu$ and $k_\mathrm{A} = k_\mathrm{B} = k$. We assume there is one copy of the genome in the cell. The reduced degradation rate is

$$\tilde{\mu} = \frac{V_\mathrm{c}}{\sqrt{K_\mathrm{b} K_\mathrm{d}}} \frac{\mu}{k}. \tag{A5}$$

For the general switch, Eqs. (8) are

$$\frac{1}{1+y^2} = \tilde{\mu} x, \quad \frac{1}{1+x^2} = \tilde{\mu} y. \tag{A6}$$

The stable fixed points are

$$(x,y) = \frac{1 \pm \sqrt{1-4\tilde{\mu}^2}}{2\tilde{\mu}}, \tag{A7}$$

where $x > y$ if the positive sign is taken for x. We see that $\tilde{\mu} < 1/2$ is required as found earlier (see Fig. 2). The unstable fixed point is

$$x = y = \frac{u - 12\tilde{\mu}^2/u}{6\tilde{\mu}} \tag{A8}$$

where

$$u^3 = 108\tilde{\mu}^2 + 12\tilde{\mu}^2\sqrt{81+12\tilde{\mu}^2}. \tag{A9}$$

For the exclusive switch, Eqs. (8) are

$$\frac{1+x^2}{1+x^2+y^2} = \tilde{\mu} x, \quad \frac{1+y^2}{1+x^2+y^2} = \tilde{\mu} y. \tag{A10}$$

The stable fixed points are

$$(x,y) = \frac{[1-2\tilde{\mu}^2 + \sqrt{1+4\tilde{\mu}^2} \pm \Delta]^{1/2}}{2\tilde{\mu}} \tag{A11}$$

where $x > y$ if the positive sign is taken for x, and

$$\Delta^2 = 2 - 12\tilde{\mu}^4 + 2(1-2\tilde{\mu}^2)\sqrt{1+4\tilde{\mu}^2}. \tag{A12}$$

One can check that $\Delta^2 > 0$ requires $\tilde{\mu} < 2/3$, as found earlier. The unstable fixed point is

$$x = y = \frac{1 + v + (1-6\tilde{\mu}^2)/v}{6\tilde{\mu}} \tag{A13}$$

where

$$v^3 = 1 + 45\tilde{\mu}^2 + 3\tilde{\mu}\sqrt{12 + 213\tilde{\mu}^2 + 24\tilde{\mu}^4} \tag{A14}$$

An expression for the total number of molecules of A in the cell which applies to both the general ($\gamma = 1$) and exclusive ($\gamma = 0$) switch is given by

$$\begin{aligned} N_\mathrm{A} &= n_\mathrm{A} + 2\,n_{\mathrm{A}_2} + 2\,n_{\mathrm{OA}_2} \\ &= \frac{x V_\mathrm{c}}{\sqrt{K_\mathrm{b} K_\mathrm{d}}} + \frac{2x^2 V_\mathrm{c}}{K_\mathrm{b}} + \frac{2(x^2 + \gamma x^2 y^2)}{1 + x^2 + y^2 + \gamma x^2 y^2}. \end{aligned} \tag{A15}$$

The total number of molecules of B is given by the same expression with x and y interchanged. This expression, together with the results above for the locations of the fixed points, is used to fill in the mean field rows in Table III. For both kinds of switch, $x = y = 1$ at the smallest value of $\tilde{\mu}$ for which bistability occurs. Therefore at this point,

$$N_\mathrm{A} = N_\mathrm{B} = \frac{V_\mathrm{c}}{\sqrt{K_\mathrm{b} K_\mathrm{d}}} + \frac{2V_\mathrm{c}}{K_\mathrm{b}} + 2\frac{1+\gamma}{3+\gamma}. \tag{A16}$$

We finally consider briefly the limit $\tilde{\mu} \to 0$, which is the limit of high expression and low degradation rates. In this limit, the stable fixed points for both exclusive and general switches converge with $x \sim 1/\tilde{\mu}$ and $y \sim \tilde{\mu}$ (or *vice versa*). However the behavior of the unstable fixed point is $x = y$ and $x \sim \tilde{\mu}^{-1/3}$ for the general switch, and $x = y$, and $x \sim 1/(2\tilde{\mu})$ for the exclusive switch.

APPENDIX B: LACK OF DETAILED BALANCE

We prove that the chemical master equation for the set of reactions in Eqs. (1) cannot satisfy detailed balance. Recall that detailed balance implies that

$$W(1 \to 2)\, P_\mathrm{S}(1) = W(2 \to 1)\, P_\mathrm{S}(2) \tag{B1}$$

where '1' and '2' indicate any two states, $W(1 \to 2)$ and $W(2 \to 1)$ are the forward and backward transition rates between the states, and P_S is the steady-state probability distribution [32]. If detailed balance holds, P_S is unique and all other probability distributions move towards P_S. For many problems, P_S is known (eg, it is the Gibbs-Boltzmann distribution). The problem is then to find a set of W which satisfies detailed balance, thus guaranteeing that the dynamics has the correct equilibrium distribution. This is the case for Metropolis Monte-Carlo schemes for example. For the Gillespie algorithm or the chemical master equation however, the W are prescribed, and we do not know necessarily know P_S.

Without prior knowledge of P_S, it would seem difficult to determine from W alone whether a system obeys detailed balance or not. However Mukamel describes a useful test [33]. Consider any cycle of states $\{1, 2, 3, \ldots, k, 1\}$. A necessary and sufficient condition

$$\begin{array}{ccc} \mathrm{OB_2} & \rightarrow & \mathrm{O+B_2} \\ \uparrow & & \downarrow \\ \mathrm{OB_2+A} & \leftarrow & \mathrm{O+B_2+A} \end{array} \qquad \begin{array}{ccc} \mathrm{OB_2} & \leftarrow & \mathrm{O+B_2} \\ \downarrow & & \uparrow \\ \mathrm{OB_2+A} & \rightarrow & \mathrm{O+B_2+A} \end{array} \tag{A4}$$

$$k_{\mathrm{off}} \times k_{\mathrm{A}} \times k_{\mathrm{on}} \times \mu_{\mathrm{A}} > 0 \qquad 0 \times k_{\mathrm{off}} \times \mu_{\mathrm{A}} \times k_{\mathrm{on}} = 0$$

FIG. 12: The fact that the products of the transition rates are different for the two cycles proves that the corresponding master equation cannot obey detailed balance. In both cases, the starting point is the state $\mathrm{OB_2}$.

for the existence of detailed balance is that

$$\begin{aligned} &W(1\to 2)\,W(2\to 3)\ldots W(k\to 1) \\ &\quad = W(1\to k)\,W(k\to k-1)\ldots W(2\to 1) \end{aligned} \tag{B2}$$

for all such cycles. To prove that a system does not obey detailed balance, it suffices to find a single counter-example.

For Eqs. (1), we can consider the cycles shown in Fig. 12. These cycles are mutual inverses, yet the corresponding products of transition rates are clearly different. This proves that the master equation corresponding to Eqs. (1) does not obey detailed balance.

It is clear that the same argument can be deployed whenever the appearance of a molecule in the system depends on the state of binding of some other molecules. This is very common, for instance it applies whenever one has gene regulation by a transcription factor. Thus the absence of detailed balance would appear to be a generic feature of any realistic biochemical reaction network.

[1] M. Ptashne and A. Gann, *Genes and signals* (Cold Spring Harbor Laboratory Press, New York, 2002).
[2] M. O. Magnasco, Phys. Rev. Lett. **78**, 1190 (1997).
[3] M. C. Eguia, S. Ponce Dawson, and G. B. Mindlin, Phys. Rev. E **65**, 047201 (2002).
[4] M. Ptashne, *A genetic switch: phage lambda and higher organisms, 2nd edn* (Blackwell, Oxford, 1992).
[5] J. J. E. Ferrell, Current Opinion Chem. Biol. **6**, 140 (2002).
[6] A. Arkin, J. Ross, and H. H. McAdams, Genetics **149**, 1633 (1998).
[7] E. Aurell and K. Sneppen, Phys. Rev. Lett. **88**, 048101 (2002).
[8] E. Aurell, S. Brown, J. Johanson, and K. Sneppen, Phys. Rev. E **65**, 051914 (2002).
[9] T. S. Gardner, C. R. Cantor, and J. J. Collins, Nature **403**, 339 (2000).
[10] P. B. Warren and P. R. ten Wolde, Phys. Rev. Lett. **92**, 128101 (2004).
[11] P. B. Warren and P. R. ten Wolde, J. Mol. Biol. **342**, 1379 (2004).
[12] Our analysis also improves on Ref. 10 in a couple of ways. Firstly, we now define $P(N_{\mathrm{A}}, N_{\mathrm{B}})$ in Fig. 3 to be a true time average, proportional to the total time the system spends in states with given values of N_{A} and N_{B}, rather than simply proportional to the number of times the system visits states with given values of N_{A} and N_{B}. Secondly, we now calculate the switch lifetime from a correlation function method described in the main text, rather than by analysing the statistics of zero-crossings of the function $N_{\mathrm{A}} - N_{\mathrm{B}}$. The zero-crossing method underestimates the lifetime because it detects not only true barrier crossing events, but also events where the system briefly visits states with $N_{\mathrm{A}} \approx N_{\mathrm{B}}$. As the switch lifetime gets longer though, the discrepancy becomes less important [31].
[13] J. L. Cherry and F. R. Adler, J. theor. Biol. **203**, 117 (2000).
[14] T. B. Kepler and T. C. Elston, Biophys. J. **81**, 3116 (2001).
[15] R. Gilmore, *Catastrophe theory for scientists and engineers* (Dover, New York, 1981).
[16] D. T. Gillespie, J. Phys. Chem. **81**, 2340 (1977).
[17] A. B. Bortz, M. H. Kalos, and J. L. Lebowitz, J. Comp. Phys. **17**, 10 (1975).
[18] R. Bundschuh, F. Hayot, and C. Jayaprakash, Biophys. J. **84**, 1606 (2003).
[19] W. Bialek, in *Advances in Neural Information Processing* **13**, Eds T. K. Leen, T. G. Dietterich and V. Tresp (MIT Press, Cambridge, 2001); see also cond-mat/0005235.
[20] C. H. Bennett, in *Algorithms for Chemical Computations*, edited by R. E. Christofferson, Am. Chem. Soc., Washington, D. C. (1977).
[21] D. Chandler, J. Chem. Phys. **68**, 2959 (1978).
[22] D. Chandler, *Introduction to modern statistical mechanics* (Oxford University Press, New York, 1987).
[23] G. M. Torrie and J. P. Valleau, Chem. Phys. Lett. **28**, 578 (1974).
[24] M. R. Evans, D. P. Foster, C. Godrèche, and D. Mukamel, Phys. Rev. Lett. **74**, 208 (1995).
[25] C. Godrèche, J. M. Luck, M. R. Evans, D. Mukamel, S. Sandow, and E. R. Speer, J. Phys. A: Math. Gen. **28**, 6039 (1995).
[26] H. H. McAdams and A. Arkin, Proc. Natl. Acad. Sci. **94**, 814 (1997).
[27] M. Thattai and A. van Oudnaarden, Proc. Nat. Acad. Sci. **98**, 8614 (2001).
[28] R. Wagner, *Transcription regulation in prokaryotes* (OUP, Oxford, 2000).
[29] C. V. Rao, D. M. Wolf, and A. P. Arkin, Nature **420**,

231 (2002).
[30] P. G. Bolhuis, D. Chandler, C. Dellago, and P. L. Geissler, Annu. Rev. Phys. Chem. **53**, 291 (2002).
[31] R. J. Allen, P. B. Warren, and P. R. ten Wolde, q-bio.MN/0406006.
[32] N. G. van Kampen, *Stochastic Processes in Physics and Chemistry* (Elsevier, Amsterdam, 2001).
[33] M. Mukamel, in *Soft and fragile matter*, Eds M. E. Cates and M. R. Evans (IOP Publishing, London, 2000).